Frontiers in Bioscience Landmark

Front. Biosci. (Landmark Ed) **2023**; 28(2): 22
https://doi.org/10.31083/j.fbl2802022

Original Research

Dietary Ochratoxin A Contamination Modulates Oxidative Stress, Inflammation Processes and Causes Fibrosis in *in vitro* and *in vivo* Lung Models

Yongfang Ou[1,†], Qiujuan Fu[1,†], Yonghua Chen[1], Liyao Lin[2], Junfeng Wang[2], Dong Wu[2], Qin Wu[2], Jianlong Xie[2,*]

[1]Pathological Diagnosis and Research Center, Affiliated Hospital of Guangdong Medical University, 524000 Zhanjiang, Guangdong, China
[2]Department of Cardiothoracic Surgery Center, Affiliated Hospital of Guangdong Medical University, 524000 Zhanjiang, Guangdong, China
*Correspondence: jlxiewy@gdmu.edu.cn (Jianlong Xie)
[†]These authors contributed equally.

Academic Editor: Soo-Jin Choi
Submitted: 29 October 2022 Revised: 1 December 2022 Accepted: 8 December 2022 Published: 2 February 2023

Abstract

Background: The prevalence of aging-related diseases has increased significantly and this imposes a burden on both families and society. The lung is one of the few internal organs that is continuously exposed to the external environment, and lung aging is associated with a number of lung diseases. Ochratoxin A (OTA) is a toxin that is widely present in food and the environment but an effect for OTA on lung aging has not been reported. **Methods**: Using both cultured lung cell and *in vivo* model systems, we studied the effect of OTA on lung cell senescence using flow cytometry, indirect immunofluorescence, western blotting, and immunohistochemistry. **Results**: Results obtained showed that OTA caused significant lung cell senescence in cultured cells. Furthermore, using *in vivo* models, results showed that OTA caused lung aging and aging fibrosis. Mechanistic analysis showed that OTA upregulated the levels of inflammation and oxidative stress, and that this may be the molecular basis of OTA-induced lung aging. **Conclusions**: Taken together, these findings indicate that OTA causes significant aging damage to the lung, which lays an important foundation for the prevention and treatment of lung aging.

Keywords: ochratoxin A; lung aging; lung fibrosis; inflammation; oxidative stress

1. Introduction

As the aging situation in the world progresses, and the prevalence of aging-related diseases has increased significantly [1], and as a result, aging has brought huge economic and social burdens to society and families [2]. It is thus important that the molecular mechanisms that drive the aging process are understood in tissues, organs and cells.

The lung is one of the few internal organs that is continuously exposed to the external environment. The impact of the environment on the structure and function of the lung largely determines its health, for example, lung is one of the organs with the highest levels of oxidative stress [3]. Aged lungs are more susceptible to damage from environmental exposures due to changes in lung function and anatomy as well as dysregulation of the lung's antioxidant defenses [4]. Lungs are frequently exposed to oxidative stress-inducing insults, such as cigarette smoke, airborne aerosols, particulates emitted by diesel fuel, and other exogenous toxins [5,6]. In addition to understanding natural lung aging, the effect of various toxins on the aging of the lungs is also a scientific problem that requires further study.

There are many environmental toxins. Ochratoxin is a toxin produced by *Aspergillus ochraceus* and several fungi belonging to the *Penicillium* genus. According to their different chemical structures, ochratoxin are usually divided into classes ochratoxin A (OTA), ochratoxin B (OTB), and ochratoxin C (OTC). Of these classes, OTA is the most toxic, is most widely encountered in the environment, and has a relative molecular mass of 403.8 kDa. OTA is highly toxic and is widely found as a contaminant in food and traditional Chinese medicines [7,8]. OTA is chemically stable and exhibits good heat resistance; thus, its chemical properties do not easily change during the process of feed conversion. Once humans or animals consume OTA-contaminated feed, OTA will be absorbed and distributed in the liver, kidney, heart, muscle, blood, and throughout the gastrointestinal system [9,10]. OTA can contaminate various food products such as wheat, peanuts, and beer.

Many countries have successively stipulated a limit for OTA in food and feed [11,12]. Several studies found that OTA has a certain level of toxicity on various tissues and organs [13,14]. Further, other studies reported that the kidney is one of the main target organs for OTA-induced toxicity [15]. Moreover, acute OTA exposure can cause cytotoxicity in organs and tissues such as the liver and gastrointestinal tract [16]. OTA has also been linked to other health challenges, such as neurotoxicity, immunotoxicity, inflammation, carcinogenicity, oxidative stress, and mitochondrial damage [17].

To date, the effect of OTA on lung aging has not been

reported, leading us to investigate the potential effects of OTA on lung aging. Findings outlined in this study show that OTA causes significant aging damage to the lung.

2. Materials and Methods

2.1 Reagents and Antibodies

OTA was purchased from Merck (CAS No.: 303-47-9, Merck Co Inc. Kenilworth, NJ, USA). Western blotting primary antibody diluent buffer (Cat no. C05-07001) was purchased from Bioss Biotechnology Co., Ltd (Beijing, China). Tris Buffered Saline with Tween 20 (TBST, Cat no. T1081), PBS phosphate buffer (Cat no. 1022), Bovine serum albumin (BSA) blocking solution (Cat no. A8020), and BCA protein assay kit (Cat no. PC0020) were purchased from Beijing Solarbio company (Beijing, China). Rabbit monoclonal β-actin antibody (cat no: ab8226, 1:1500 dilution), anti-p16 antibody (cat no: ab189034, 1:2000 dilution), anti-p21 (cat no: ab109199, 1:1000 dilution), Ki67 (cat no: ab15580, 1:1000 dilution) and α-SMA (cat no: ab5694, 1:1500 dilution) were purchased from Abcam (Cambridge, UK). Horseradish peroxidase (HRP)-conjugated goat anti-rabbit IgG was purchased from Beyotime Biotechnology Co., Ltd (Shanghai, China). Polyvinylidene fluoride (PVDF) membrane (0.22 μm pore size, Cat no. GVWP09050) was obtained from Millipore (Boston, MA, USA). Fetal bovine serum (Cat no.12484028) and Dulbecco's Modification of Eagle's Medium (DMEM) culture medium (Cat no. 11965092) were purchased from Thermo Fisher Company (Shanghai, China). Mouse IL-1β ELISA kit (Cat no. SEKM-0002) and mouse IL-6 ELISA (Cat no. SEKM-0007) were purchased from Solarbio Biotechnology Co., Ltd (Beijing, China). Total Superoxide Dismutase (T-SOD, Cat no. BC0170), MDA (malonaldehyde, Cat no. BC0025), and GSH (glutathione, Cat no. BC1175) kits were purchased from from Solarbio Biotechnology Co., Ltd (Beijing, China).

OTA was purchased from Merck (CAS No.: 303-47-9) (Shanghai, Chian). Western blotting primary antibody diluent buffer was purchased from Beyotime Biotechnology Co., Ltd (Shanghai, China). 10$\times$ TBST, PBS phosphate buffer (0.01 M pH 7.2–7.4), Sodium Dodecyl Sulfate PolyAcrylamide Gel Electrophoresis (SDS–PAGE) electrophoresis solution, BSA blocking solution, BCA protein assay kit, 5X SDS–PAGE protein loading buffer, hematoxylin and eosin dye were purchased from Beijing Solarbio company (Beijing, China). Rabbit monoclonal β-actin antibody (cat no: ab8226, 1:1500 dilution), anti-p16 antibody (cat no: ab189034, 1:2000 dilution), anti-p21 (cat no: ab109199, 1:1000 dilution), Ki67 (cat no: ab15580, 1:1000 dilution) and α-SMA (cat no: ab5694, 1:1500 dilution) were purchased from Abcam (Cambridge, UK). HRP-conjugated goat anti-rabbit IgG was purchased from Beyotime Biotechnology Co., Ltd (Shanghai, China). PVDF membrane (0.22 μm pore size) was obtained from Millipore (MA, USA). A protein extraction kit was purchased from Jiangsu Kaiji Biotechnology Co., Ltd (Nanjing, China). Toluidine blue was purchased from Beijing Biotechnology Co., Ltd (Beijing, China). Fetal bovine serum and DMEM culture medium were purchased from Thermo Fisher Company (Shanghai, China). Mouse IL-1β ELISA and mouse IL-6 ELISA kits were purchased from Solarbio Biotechnology Co., Ltd (Beijing, China). A T-SOD, MDA, and GSH kits were purchased from Nanjing Jiancheng Biotechnology Co., Ltd (Nanjing, China).

2.2 Cell Culture

TC-1 and MLE-12 murine lung epithelial cell lines were cultured in DMEM supplemented with 10% fetal bovine serum (FBS) at 37 °C in an incubator with a 5% CO_2 atmosphere.

2.3 Cell Passaging

Cell density was observed and monitored under a microscope. When the cell density was greater than 75%, the medium in the cell culture flask was discarded and washed three times with normal saline. Cells were digested using trypsin and digestion, serum-containing DMEM medium was added and the cell suspension was inoculated into cell culture plates.

2.4 Animal Treatment

All animal procedures were reviewed and approved by the affiliated Hospital of Guangdong Medical University (IACUC-2210-A061). Forty (40) male C57 mice (body weight 20–22 g, 8 weeks old) were divided into a control group and three OTA groups with 10 mice in each group. Mice were treated with OTA for 30 days by gavage. In the control group the mice were treated with 0.1 mL olive oil by gavage every day, and then 0.1 mL of $NaHCO_3$ was given 2 h later. In the OTA groups the mice were treated with 0.1 mL of olive oil by gavage every day, and then treated with low-dose (1 mg/kg), medium dose (5 mg/kg), or high-dose OTA (10 mg/kg) 2 h later.

2.5 Western Blotting

Cells were washed three times with PBS, cell lysis buffer was added, and the plate placed on ice for 30 min. Cells were subsequently collected and transferred into 1.5 mL microfuge tubes. The protein lysates were centrifuged at 12,000 rpm for 15 min, and the cleared supernatant was transferred into another microfuge tube. 30 μg of protein was subjected to SDS–PAGE, protein samples were electrotransferred to PVDF membranes. PVDF membranes were subsequently blocked in 5% skim milk at room temperature for 1 h. Primary antibodies were added and incubated overnight at 4 °C with shaking. After washing the membrane three times with TBST, secondary antibody diluted in 2% skim milk was added and incubated at room temperature for 2 h. After washing the membrane three times with TBST (10 min/times), enhanced chemiluminescence

(ECL) solution was added to the PVDF membrane and protein bands visualized using a Bio-Rad ChemiDoc™ XRS system (ImageLab developed by Bio-rad company, Hercules, CA, USA).

2.6 Mouse Lung Sample Collection

Following blood collection, the mice were sacrificed using the cervical dislocation method. The mice were subsequently fixed on a wooden board, and the abdominal and thoracic cavity were opened from bottom to top using surgical scissors. After opening the thoracic cavity, the intact lungs were carefully extracted and weighed on an analytical balance. Following this, the lungs were divided into two pieces, one piece was placed in 4% polymethanol tissue fixative for immunohistochemistry and the second piece was washed with sterile normal saline, after which it was blotted dry with filter paper and then placed in a cryopreservation tube and stored at –80 °C for subsequent detection of biochemical indicators and protein content.

2.7 Calculation of the Mouse Lung Coefficient

Following dissection of whole mouse lungs, lungs were weighed, and a mouse lung coefficient was calculated per the formula: mouse whole lung weight (g)/mouse body weight (g) $\times$ 100%.

2.8 Hematoxylin and Eosin (H&E) Staining

The lung tissues of mice in each group were fixed in 4% paraformaldehyde solution. The fixed tissues were dehydrated, embedded, and sectioned on a rotary microtome. The tissue sections were stained with hematoxylin for 10–20 min, rinsed with tap water for 1–3 min, and destained with hydrochloric acid alcohol for 5–10 seconds, after which the tissue sections were rinsed with tap water for 1–3 min. Finally, the tissue sections were placed into warm water followed by placing into 85% alcohol for 3–5 min, staining with eosin for 3–5 min, and dehydrated with alcohol. Finally, the slices were deparaffinized with xylene, mounted with neutral gum, and then placed under a microscope to observe the tissues.

2.9 Masson Staining

Tissue sections were subjected to Masson staining according to the manufacturer's instructions. In brief, tissue sections were stained with Weigert's iron hematoxylin staining solution for 5–10 min, and sections were then soaked in a 0.2% glacial acetic acid aqueous solution for 5–10 min. The sections were de-stained using 1% aqueous phosphotungstic acid (3–5 min). After this, the sections were stained with toluidine blue for 5 min. After staining, the sections were washed with 0.2% glacial acetic acid aqueous solution for 5–10 min. After the sections were soaked and washed, they were deparaffinized with a series of 95% ethanol, absolute ethanol, and xylene. Finally, the sections were sealed with neutral gum and then observed under a microscope.

2.10 Immunohistochemical Staining

Tissue sections were blocked using 5% BSA in a –37 °C incubator for 1 h. After washing three times with PBS, the blocking solution was discarded, and the primary antibody, diluted in 3% BSA, was added dropwise until the tissue was covered. The tissue sections was incubated at –4 °C overnight and subsequently the tissues were washed three times with PBS. After this, a solution containing HRP-conjugated secondary antibody was added dropwise to the tissues and they were incubated at RT for 1 h. After three washes with PBS, DAB (3,3'-Diaminobenzidine Tetrahydrochloride) was added to the tissue, and tap water was used to stop the reaction when the sections were sufficiently developed, and subsequently observed under a microscope.

2.11 Immunofluorescence Staining

Tissue sections were blocked with 5% BSA and incubated in a 37 °C incubator for 1 h. After the blocking solution was removed, primary antibody diluted in 5% BSA was added dropwise to cover the tissues, and the sections were incubated at 4 °C for overnight. After washing with PBS three times, fluorescently-labeled secondary antibody diluted in 3% BSA was added dropwise, and the tissue was covered and incubated in a 37 °C incubator for 2 h. After three washes with PBS, the tissue samples were mounted with glycerol and the tissues were examined by fluorescence microscopy.

2.12 Assessment of Oxidative Stress

Cells in logarithmic growth were seeded in 6-well cell culture plates, and OTA was added and incubated at different time points. After incubation, the medium was discarded, the cells were washed three times with PBS, and collected into centrifuge tubes. After the samples were centrifuged, the supernatant was discarded, and cells were sonicated. The supernatant of the cells was placed in a 96-well plate, and various reagents were added in sequence according to the manufacturer's instructions. The samples were then tested for indicated oxidative stress indicators using commercial SOD (Cat no. BC0170, Solarbio Science & Technology Co., Ltd, Beijing China), MDA (Cat no. BC0025, Solarbio Science & Technology Co., Ltd, Beijing, China), and reactive oxygen species (ROS, Cat no. S0033S, Beyotime Biotechnology company, Shanghai, China) kits.

2.13 MTT Viability Assay

Lung cells in the logarithmic growth phase were plated in 96-well cell culture plates at a density of 1.5 $\times$ 10^4 cells/well, and cultured for an additional 24 h. Following this, indicated concentrations of OTA were added and the cells further incubated for 24–48 h. After this the cells were washed, MTT (3-(4,5-Dimethylthiazol-2-yl)-2,5-diphenyltetrazolium bromide) solution was added (fi-

nal concentration: 0.5 μg/mL), and the plates incubated for 4 h. After the addition of DMSO (Dimethyl sulfoxide), absorbance was measured at 450 nm using a microtiter plate reader (ST-360, Thermo Fisher, Houston, TX, USA).

2.14 Sa-β-Gal Staining

Cells in the logarithmic phase were seeded into 6-well cell culture plates, indicated concentrations of OTA were added, and the cells were incubated for 24 h. After this, the supernatant was discarded, cells were washed with PBS, 1 mL of PFA was added to each tube, and the cells were fixed for 15 min at RT (room temperature). Following this, the fixative was discarded, and the cell samples were washed with PBS. After adding 1 mL of staining working solution to each well, plates were covered in parafilm and incubated overnight in a 37 °C incubator. Five fields of view were randomly selected for each sample and ImageJ software (version: 1.8.0, developed by National Institutes of Health, LOCI, University of Wisconsin, Madison, WI, USA) was used to count senescent cells.

2.15 Detection of Inflammatory Markers in Mouse Lung Tissue

Freshly prepared lungs were homogenized with a tissue homogenizer. The homogenate was placed in a benchtop refrigerated centrifuge and centrifuged at 3000 rpm for 20 min. The supernatant was collected after centrifugation. TNF-α (PT513, Solarbio Science & Technology Co., Ltd, Beijing, China), IL-1β (SEKM-0002, Solarbio Science & Technology Co., Ltd, Beijing, China) and IL-6 (SEKM-0007, Solarbio Science & Technology Co., Ltd, Beijing, China) assays were performed according to the instructions of the ELISA kit.

2.16 Statistical Analysis

Data are expressed as the mean $\pm$ standard deviation. Statistical analysis was performed using SPSS 22.0 software (IBM Corp., Chicago, IL, USA). All data were analyzed by ANOVA and multiple comparisons using Fisher's Least Significant Difference (LSD) test. $p < 0.05$ is used to indicate a significant difference; $p < 0.01$ indicates an highly significant difference.

3. Results

3.1 OTA Induces Lung Cell Senescence.

Previous studies found that OTA causes cytotoxicity [18]. However, in the current study, we analyzed the effect of OTA on lung cell. MTT assays were used to determine the effect of different concentrations of OTA on the viability of cultured lung cells. The results indicated that the effect of OTA on the viability of lung cells was not apparent at low OTA concentrations. However, when OTA concentration was increased, cell viability was significantly decreased (Fig. 1A). Based on these MTT assay results, we selected three concentrations of OTA, 1, 5 and 10 μM, for use in the outlined experiments.

Senescence-associated β-galactosidase (SA-β-Gal) is one of the most important markers of senescent cells. As shown in Fig. 1B, with increasing OTA concentration, the percentage of Sa-β-gal-positive cells increased. Furthermore, the expression of Ki67 was also significantly downregulated (Fig. 1C). Moreover, cell cycle distribution showed that OTA resulted in significant cell cycle arrest (Fig. 1D).

3.2 Effect of OTA on the Expression of Senescence-Related Marker Molecules p16, p21, and p53

P16 and p21 are cell cycle regulatory proteins, and the expression of these proteins is significantly upregulated in senescent cells. In the current work, the expression of p16, p21, and p53 was evaluated by western blotting. The results showed that OTA treatment increased the protein expression of each of these proteins compared to the control treated cells (Fig. 2).

3.3 The Effect of OTA on Oxidative Stress

We next evaluated the effect of OTA on oxidative stress. We found that the levels of reactive oxygen species (ROS) and malondialdehyde (MDA) in the cells were significantly increased compared with those in the control group. In contrast, the levels of SOD, CAT and GSH were significantly downregulated. Compared with the control group, 1 μM OTA increased ROS/MDA levels to 12.8% and 21%; 5 μM OTA increased ROS/MDA levels to 26.8% and 37%; and 10 μM increased ROS/MDA levels by 62.5% and 74.5%, respectively (Fig. 3A). In addition, these various concentrations of OTA significantly decreased the levels of SOD, GSH and CAT. Furthermore, OTA significantly downregulated the expression of Nrf2 (Nuclear Factor erythroid 2-Related Factor 2), HO-1 (heme oxygenase 1) and MnSOD (manganese superoxide dismutase) (Fig. 3B).

3.4 The Effect of OTA on Lung Cell Inflammation

We investigated the effect of OTA on the secretion of senescence-associated secretory phenotype (SASP) factors in cultured lung cells. SASP is one of the key phenotypic features of senescent cells, and includes proinflammatory factors, such as IL-6, IL-1β and TNF-α, CXCL1 chemokine, and MMP-1 metalloproteinase. Here, we analyzed the effect of OTA on inflammation in lung cells, and the results showed that the expression of each of these inflammation-related factors was significantly increased, indicating that OTA increased the inflammation of lung cells (Fig. 4).

3.5 Effects of OTA on Body Weight and Lung Coefficient

As shown in Fig. 5A, the average weight of mice in each of the OTA-treated groups was lower than that in the control group. Specifically, the average weight of mice in the 5 mg/kg and 10 mg/kg OTA groups was significantly

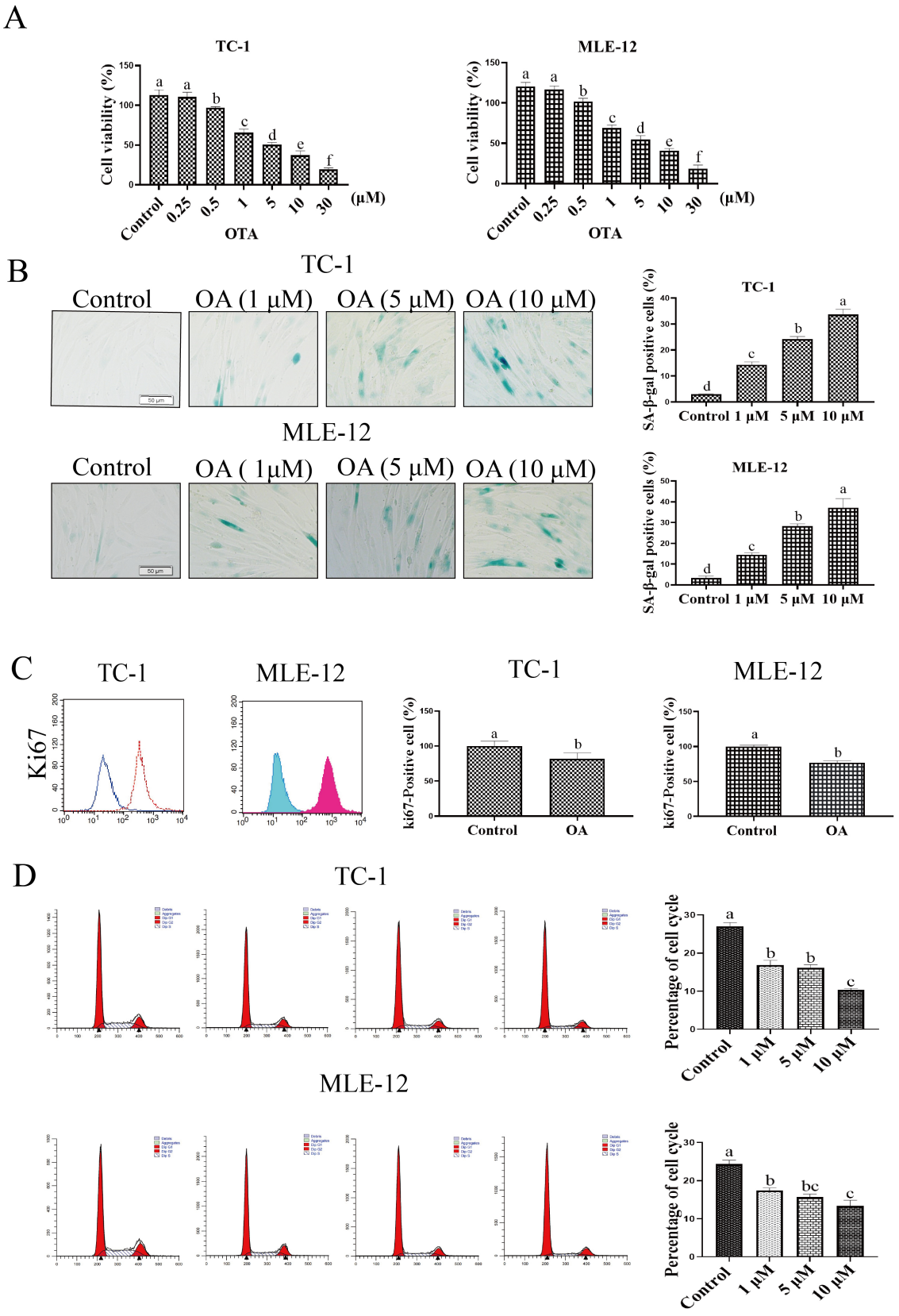

Fig. 1. OTA induced Lung Cell Senescence. (A) Effect of OTA treatment on cell viability. (B) OTA treatment increased *ratio* of SA-β-Gal-positive ratio. (C) OTA treatment reduced the expression of Ki67. (D) OTA caused cell cycle arrest. Different lowercase letters indicate significant differences ($p < 0.05$).

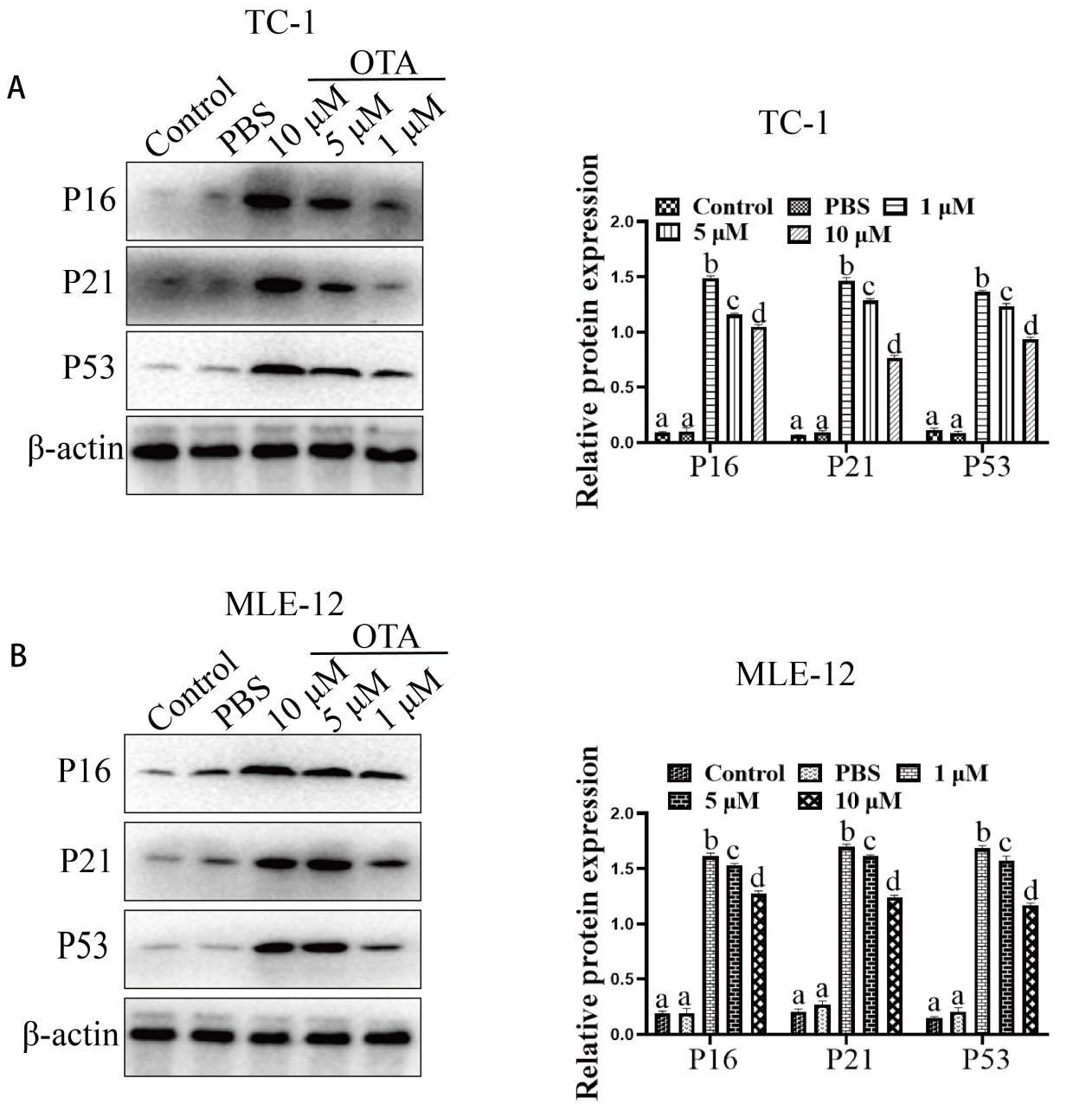

Fig. 2. Effect of OTA on the expression of senescence-related marker molecules. Effect of OTA on p16/p21/p53 protein expression in TC1 (A) and MLE-12 (B). The protein samples were subjected to SDS–PAGE, Western-blot analyses were them performed. Different lowercase letters indicate significant differences ($p < 0.05$).

reduced compared with the control group. Further, as indicated in Fig. 5B, the lung weight/body weight ratio in the OTA-treated groups was much higher than that in the control group.

3.6 Histochemical Staining of Lungs from OTA-Treated Mice

OTA-induced changes in mouse lung tissues were observed by Hematoxylin and Eosin (H&E) staining. In the control group, the structure of the bronchial branches in the lungs at all levels was typical, the bronchial ciliated epithelial cells in the lungs were neatly arranged, and there was no apparent inflammatory infiltration. In the low-dose OTA treatment group, the structure of the bronchial branches in the lungs was typical, and mild alveolar inflammation was observed in the lungs. In the moderate and high dose OTA groups, moderate alveolar inflammation was observed in the lungs, with inflammatory infiltration of many macrophages and lymphocytes. As illustrated in the histograms, inflammatory cells in the lungs of mice in the high-dose OTA group covered 30% of the total lung area. This may potentially lead to functional necrosis of the lungs (Fig. 6).

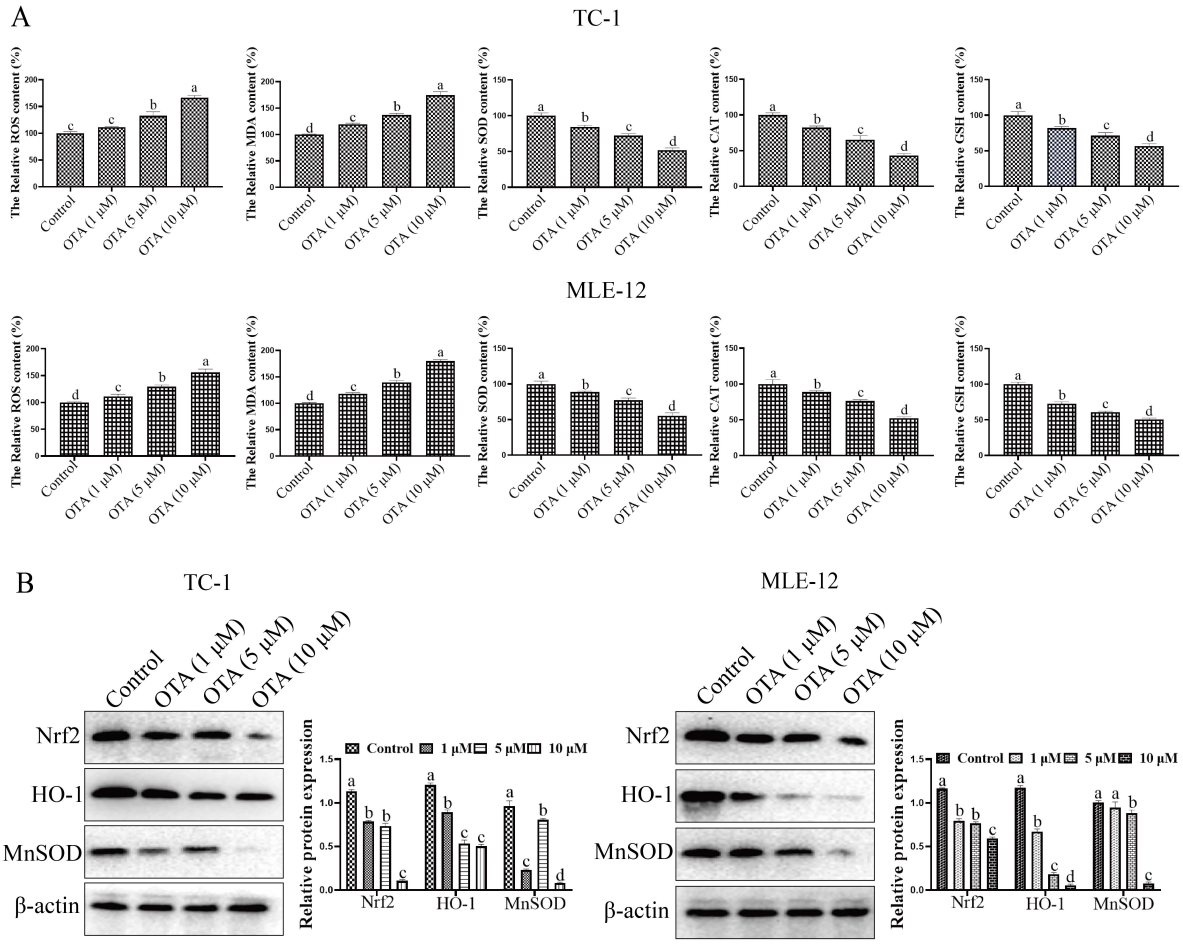

Fig. 3. Effect of OTA on oxidative stress. (A) Effects of OTA on oxidative stress (ROS, MDA, SOD, CAT and GSH) on TC-1 and MLE-2 cells. Cells in the logarithmic growth phase were seeded in 6-well cell culture plates, and OTA (1, 5 and 10 μM) was added, respectively. (B) Effects of ochratoxin A on Nrf2, HO-1 and MnSOD protein expression. The protein samples were subjected to SDS–PAGE, after which the protein samples were transferred to PVDF membranes. After western-blot, Blots were exposed using the Bio-Rad ChemiDocTM XRS system. Different lowercase letters indicate significant differences ($p < 0.05$).

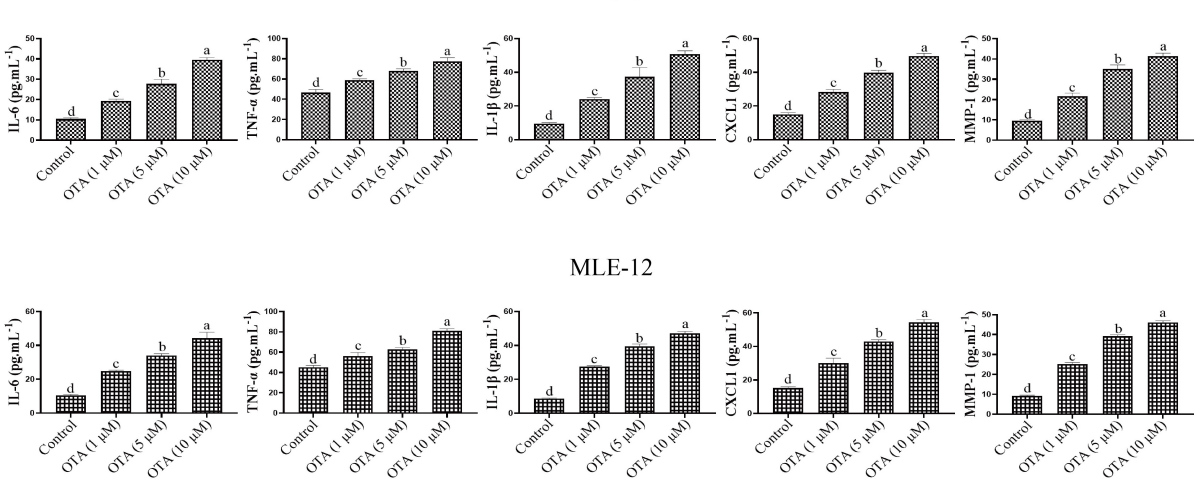

Fig. 4. Effects of OTA on lung cell inflammation. ELISA kit (TNFα, IL-6) was used to detect the effect of OTA on lung cell inflammation according to the kit instructions (n = 5). Different lowercase letters indicate significant differences ($p < 0.05$).

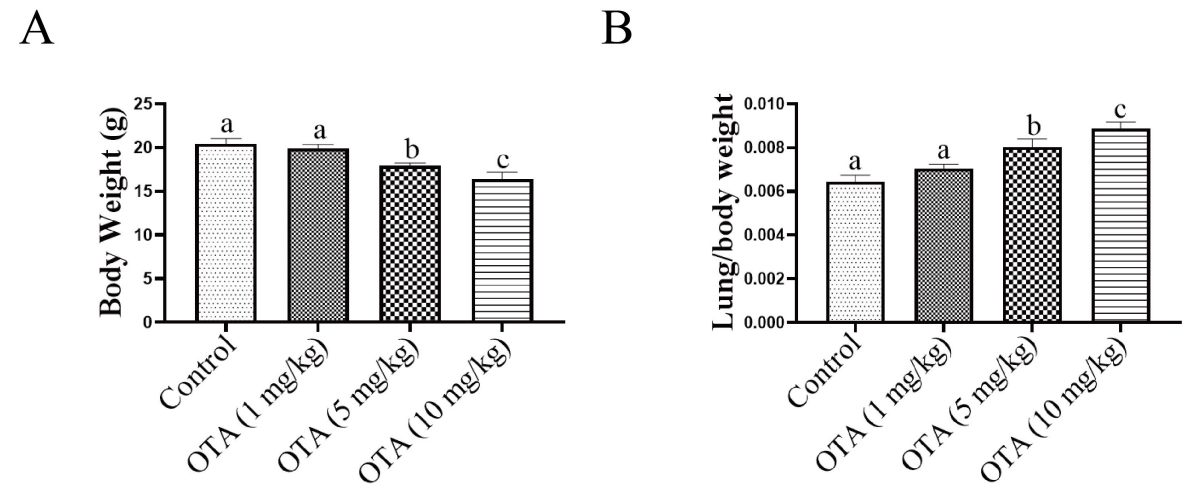

Fig. 5. Effects of OTA on body weight and lung coefficient. (A) Effect of OTA on average body weight (n = 10). (B) The ratio of lung weight/body weight was increased in the OTA group (n = 10). Different lowercase letters indicate significant differences ($p < 0.05$).

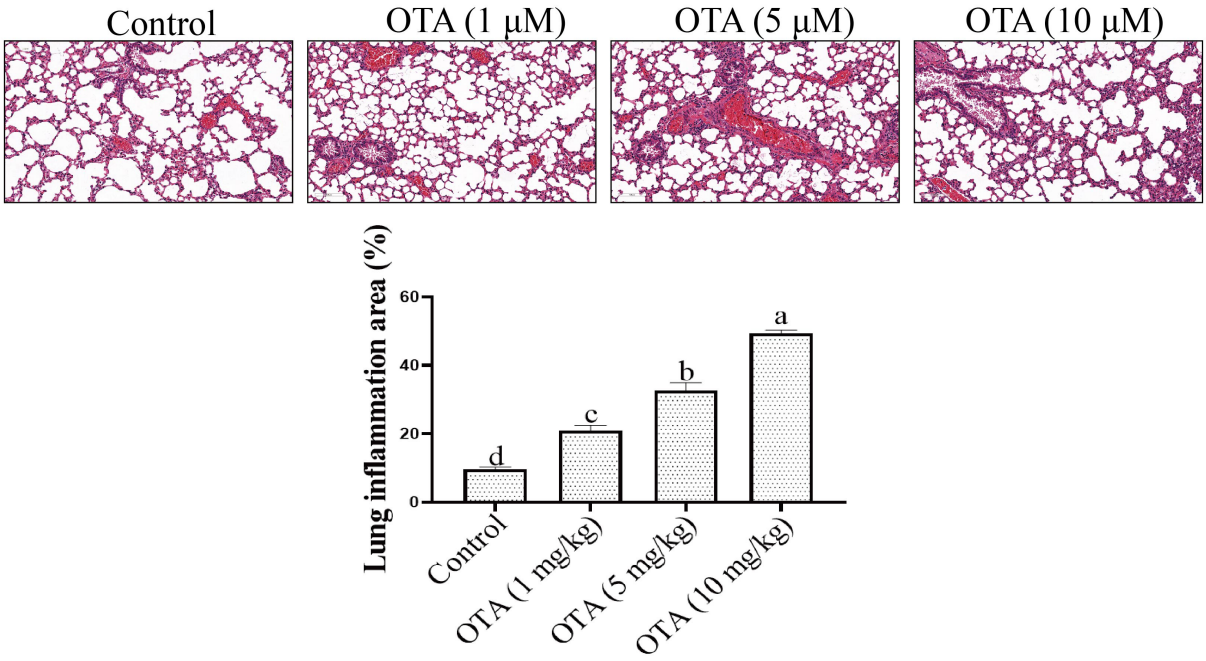

Fig. 6. Analysis of lung tissue by HE staining. The lung tissues of mice in each group were fixed in 4% paraformaldehyde solution. The sections were stained with hematoxylin. Different lowercase letters indicate significant differences ($p < 0.05$).

3.7 OTA Treatment Results in Lung Tissue Aging

We next analyzed the effects of OTA on lung tissue aging. Sa-β-gal staining showed that staining was significantly increased, indicating that the lungs displayed significant senescence (Fig. 7A). Further, the expression of p16 and p21 was also significantly increased compared to that in the control group (Fig. 7B). and the expression of the proliferation marker Ki67 was increased (Fig. 7C). These findings suggest that OTA induces lung aging.

3.8 The Effect of OTA on Lung Fibrosis

Fibrosis is also an important manifestation of organ aging [19]. Masson staining showed that the bronchial branches of the lung in the control group were relatively normal with no alveolar wall or bronchial wall fibrosis evident, nor was obvious damage to the lung tissue structure observed. Moderate pulmonary fibrosis, alveolar wall, and bronchial wall fibers were observed in the OTA group. The degree of collagenization was also found to be increased, and collagen fibers were raised significantly (Fig. 8A). Further study showed that the expression of α-SMA (alpha smooth muscle actin) was clearly elevated compared with that in the control group (Fig. 8B).

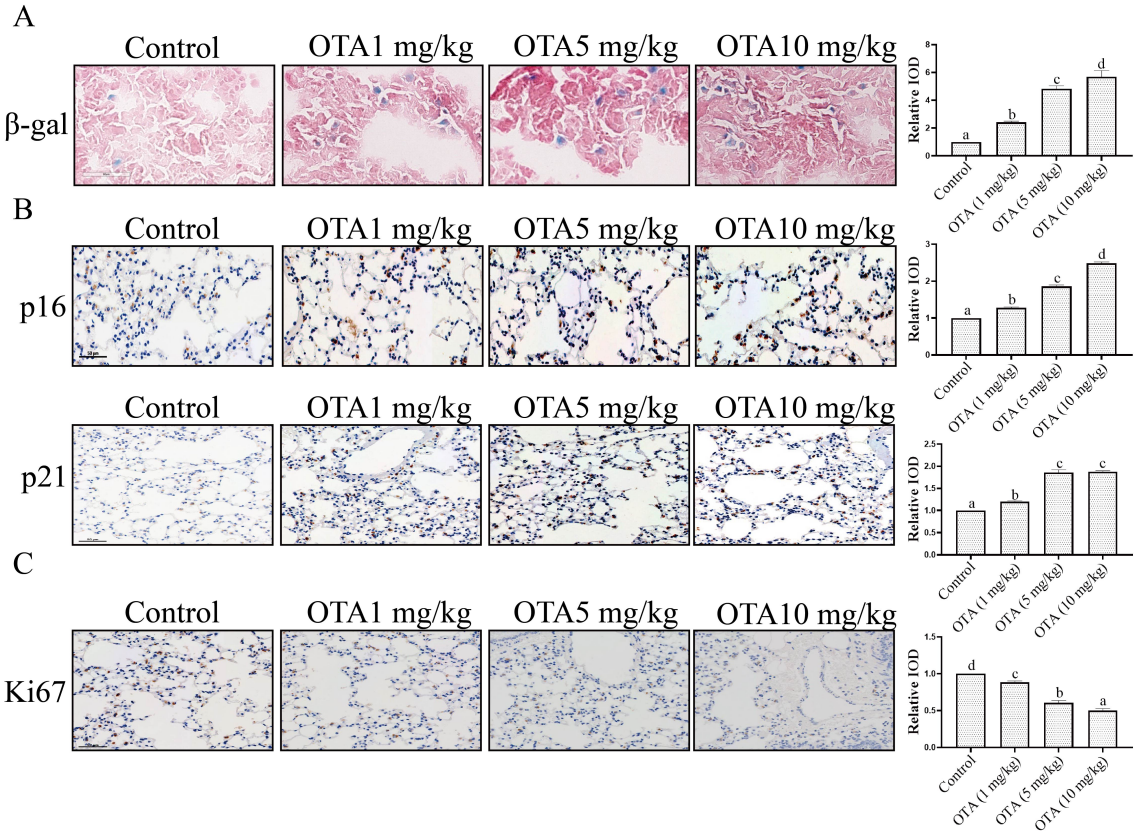

Fig. 7. Effect of OTA treatment on lung tissue aging. (A) Analysis of lung tissue aging by Sa-β-gal staining. (B) The effect of OTA on p16 and p21. (C) Effect of OTA on Ki67. The integrated optical density (IOD) values of each slide (tissue) was obtained with the software Image-Pro Plus 6.0. Different lowercase letters indicate significant differences ($p < 0.05$).

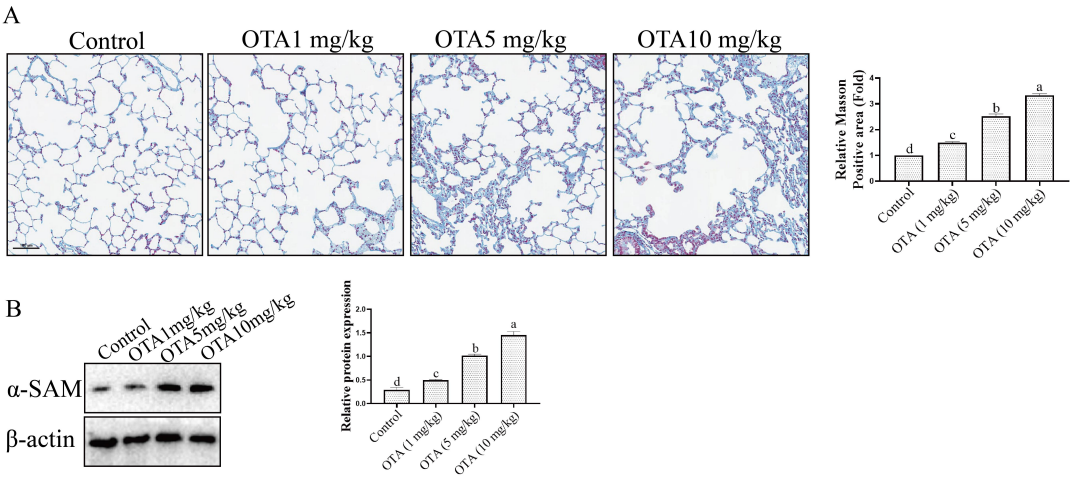

Fig. 8. Effect of OTA on Lung Fibrosis. (A) Analysis of fibrosis in lung tissue by Masson staining. (B) Effect of OTA on α-SMA expression. The protein samples were subjected to SDS–PAGE and Western-blot. Blots were exposed using the Bio-Rad ChemiDocTM XRS system. Different lowercase letters indicate significant differences ($p < 0.05$).

3.9 OTA Causes Increased Oxidative Stress in the Lungs in vivo

As shown in Fig. 9A, the MDA and ROS levels in the control group were much lower than those in the OTA-treated groups. Additionally, Fig. 9B illustrates that the SOD content in the control group was much higher than that in the OTA group. Similarly, the contents of GSH and CAT in the control group were much higher than those in the OTA group. These findings indicated that OTA exposure results in severe oxidative stress. We further analyzed

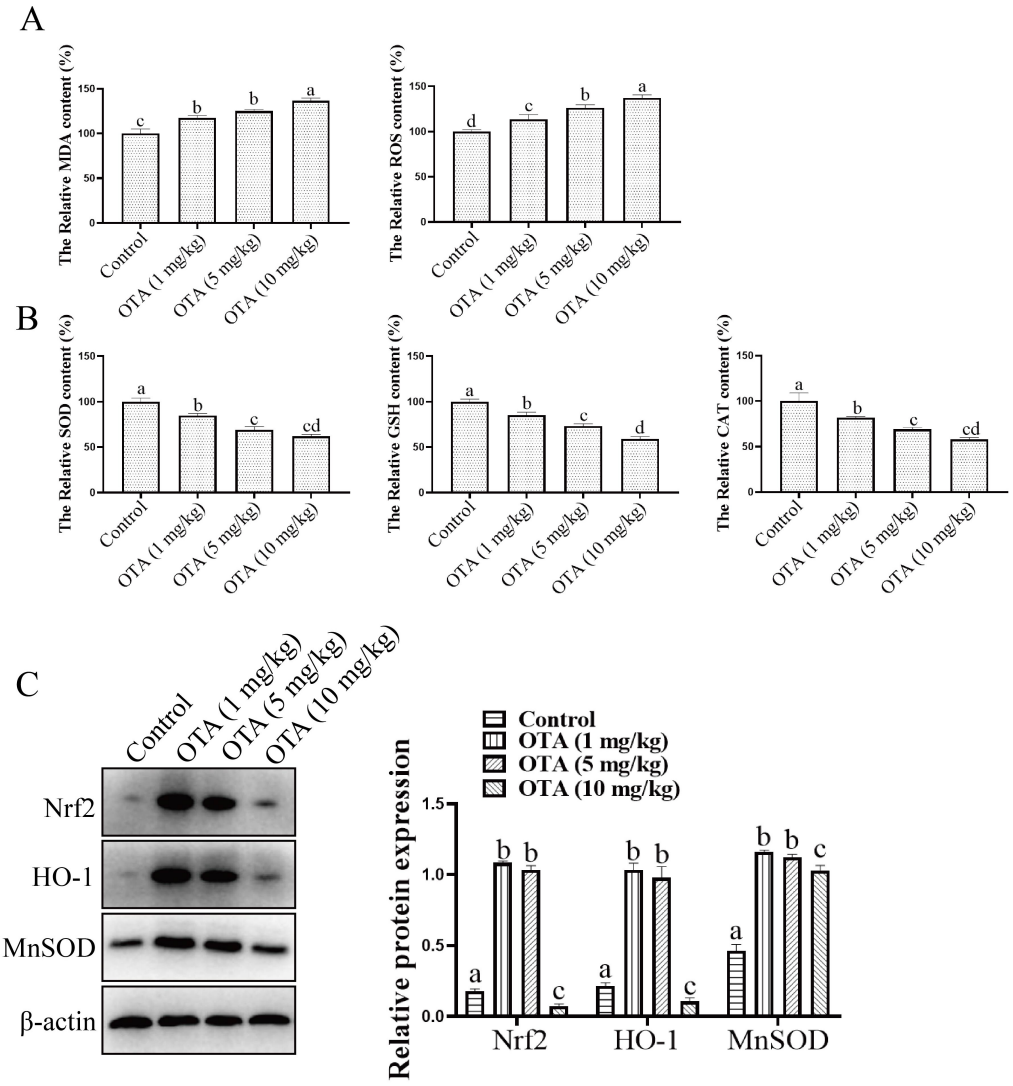

Fig. 9. Effect of OTA on oxidative stress. (A,B) Effects of OTA on oxidative stress-related protein expression. (C) Effects of OTA on the expression of Nrf2, HO-1 and MnSOD. The protein samples were subjected to SDS–PAGE and Western-blot. Blots were exposed using the Bio-Rad ChemiDocTM XRS system. Different lowercase letters indicate significant differences ($p < 0.05$).

the changes in Nrf2, HO-1 and MnSOD expression in mice lungs *in vivo*. As illustrated in Fig. 9C, compared with the control group, the expression of Nrf2 in the OTA group was obviously lower as were the expression levels of HO-1 and MnSOD in OTA-treated mouse lungs when compared to the control group.

3.10 OTA Exposure Results in Lung Inflammation

We determined the effect of OTA on lung inflammation by measuring inflammatory markers such as IL-1β, IL-6 and TNFα. As shown in Fig. 10A, when OTA-treated mice were compared with those in the control group, the levels of TNFα, IL-1β and IL6 in the OTA group were found to be clearly elevated. In addition, histochemical analysis showed that the inflammatory damage caused by OTA was evident (Fig. 10B).

Additionally, TLR4, MyD88 and NF-κB expressions were analyzed. Fig. 10C indicates that the expression of TLR4 in the OTA-treated group was higher than that in the control group, and, similarly, the expression levels of MyD88 and NF-κB were much higher than the levels observed in the control group.

4. Discussion

Aging refers to the process in which the functions of tissues and organs of the body gradually weaken with time [18]. Aging is not only a natural physiological phenomenon of the human body, but also is a result of pathological changes within the body. At present, nearly 100 countries and regions around the world have entered an aging society status, and this has brought significant medical and social burdens [20]. The lung is the principal respiratory organ in the body and is one of the few organs that is in contact with the outside air and lung aging is one of the

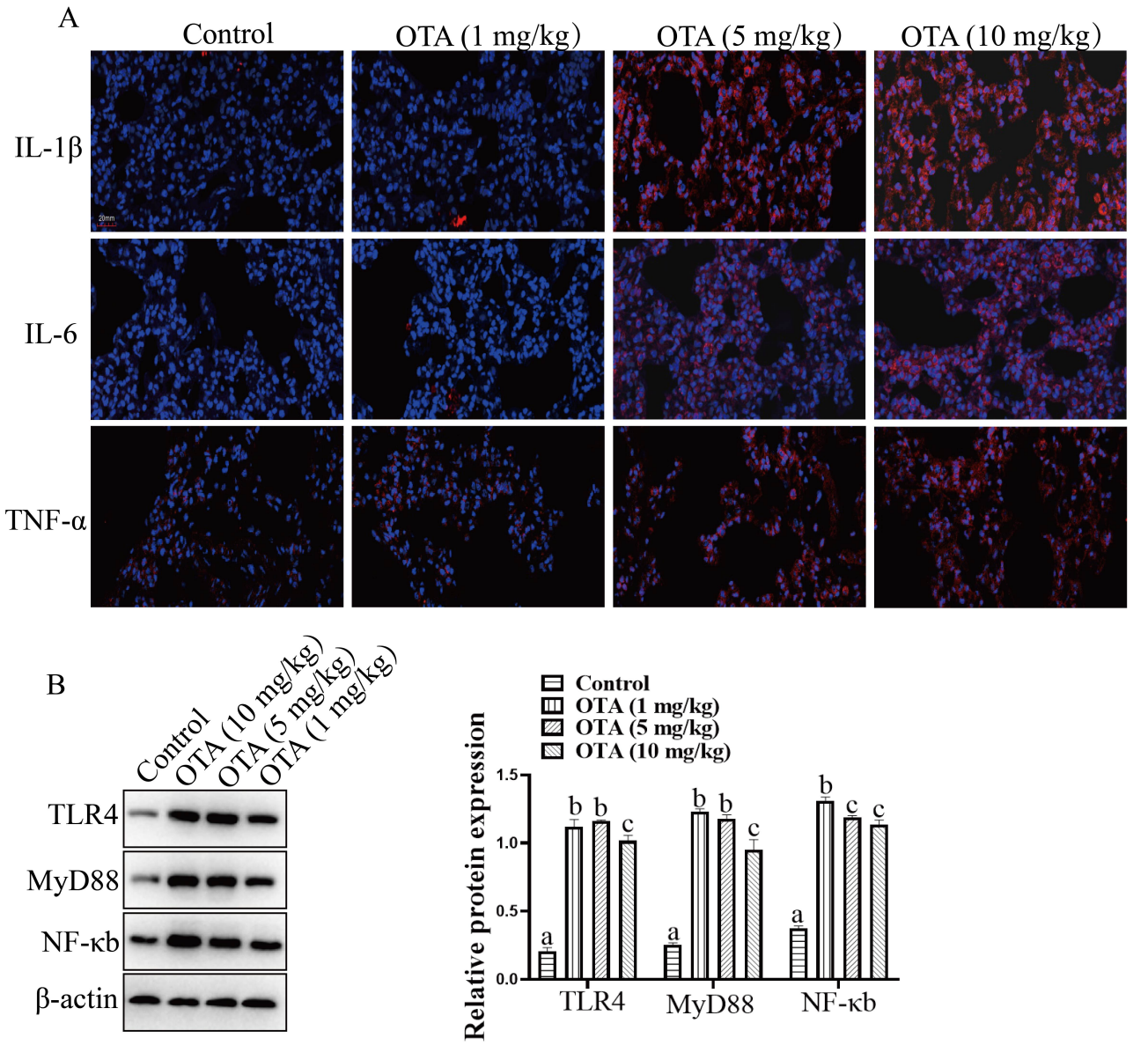

Fig. 10. OTA exposure induced Lung Inflammation. (A) Effects of OTA on IL-1β, IL-6 and TNFα. Histochemical analysis of IL-1β and IL-6 expression. (B) Effects of OTA on the TLR4/MyD88/NF-κB signaling pathway protein expressions. The protein samples were subjected to SDS–PAGE and Western blot. Blots were exposed using the Bio-Rad ChemiDocTM XRS system. Different lowercase letters indicate significant differences ($p < 0.05$).

foundations of various lung diseases. Ochratoxin is a toxin produced by *Aspergillus ochraceus* and several *Penicillium sp*. fungi, and OTA is secondary metabolite [21]. In the current study, we explored the effect of OTA on lung tissue aging, and the results showed that OTA led to rapid lung aging.

The process of cellular senescence was first proposed by Hayflick and Moorhead in 1961 [22]. Cellular senescence is currently divided into two types, specifically, replicative senescence with telomere attrition and stress-induced premature senescence without telomere involvement [23]. Cell aging is a double-edged sword with senescent cells having a variety of beneficial functions for organisms such as prevention of tumorigenesis, promoting tissue remodeling and repair, and functioning in a positive regulatory role in growth processes. However, excessive and abnormal accumulation of senescent cells in tissues negatively affects tissue regeneration capacity and results in a pre-inflammatory environment that contributes to the development and progression of various aging-related diseases such as cancer [24]. Conceptually, cellular senescence refers to cell cycle arrest induced by various stressors [25]. During the pathological process of aging, senescent cells accumulate in various tissues and increase the incidence of aging-

related diseases [26]. In this work, to verify whether OTA can induce senescence in the lung, we detected four typical senescence-related indicators, including Sa-β-gal, cell cycle, p16 and p21, and found that OTA treatment increased Sa-β-gal activity and elevated the expression of p16 and p21. Furthermore, using an *in vivo* model, we also found that OTA induced lung aging.

Senescence-associated secretory phenotype (SASP) is a general term for the secretion of a series of cytokines, such as proinflammatory factors, chemokines, and proteases, secreted by senescent cells. SASP is a double-edged sword that positively regulates immune response, cell growth, or cell differentiation in normal cells and promotes tumor migration, proliferation, invasion, and angiogenesis in human malignancies, and that this can ultimately lead to tumor metastasis [27]. Moreover, the proinflammatory effect of SASP is part of the body's normal repair response, protecting the body from bacterial and viral infections, as well as harmful environmental factors. SASP also has important roles in activating the immune system, promoting wound healing, and promoting embryonic development. However, with age, under the influence of various factors, such as the decline in the body's immune function, autophagy dysregulation, and telomere deletion, senescent cells accumulate in the body, resulting in an increase in the level of inflammatory factors and promoting the occurrence of disease. Therefore, the SASP secreted by senescent cells is not only a hallmark aging but also a predisposing factor for various age-related diseases. In the current study, using both *in vitro* and *in vivo* models, we found that OTA led to an increase in the level of inflammatory factors. *In vivo*, OTA caused severe inflammatory damage and consistent with this finding, we also noted that the signaling pathways of inflammatory factors were also significantly enhanced in the OTA-treated animals.

According to the free radical theory of aging, organisms will produce a large number of free radicals and reactive oxygen species (ROS) causing oxidative damage to nucleic acids, proteins, and lipids [28,29]. Various antioxidant defense systems exist in the lungs, such as superoxide dismutase (SOD), glutathione peroxidase, catalase, metal-binding proteins, vitamins, and surfactants, which serve to mitigate oxidative damage. OTA exists widely in life and when it enters the body, OTA promotes production of a large amount of free radicals and reactive oxygen species. In the current study, we found that OTA can cause severe oxidative damage to the lungs of mice and induced fibrosis.

Recent studies have reported that OTA could induce oxidative stress in a variety of different cellular and tissue models [19,30–35]. It has been reported that OTA-induced oxidative stress [19,31,32], and Curcumin could relieve OTA-induced hepatotoxicity and nephrotoxicity.

How is OTA transported in the circulatory system as a food-derived toxin? It has been shown that when OTA enters the circulatory system for transport to cells of all organs. It is quickly distributed in the plasma and reversibly bound to albumin, which transports OTA to various organs and tissues in the body [36].

5. Conclusions

In conclusion, we studied the potential effects of OTA on lung aging damage. First, we found that OTA caused significant cultured lung cell senescence *in vitro*. Second, using *in vivo* models, results showed that OTA caused lung aging and fibrosis. Additionally, mechanistic studies have shown that OTA upregulates the levels of inflammation and oxidative stress proteins, which may be a potential mechanism for the observed OTA-induced lung aging. The current work lays an important foundation for the relationship between OTA and lung aging.

Availability of Data and Materials

Data can be obtained upon reasonable request to the corresponding author.

Author Contributions

YFO and JLX—conceived the study, designed the experiments, per-formed the experiments and analyzed data. QW, YHC and QJF—drafted the manuscript. LYL, JFW and DW—revised the manuscript. All authors approved the final manuscript.

Ethics Approval and Consent to Participate

All animal procedures were reviewed and approved by the affiliated Hospital of Guangdong Medical University (IACUC-2210-A061).

Acknowledgment

Not applicable.

Funding

This research was funded by Guangdong Medical University Youth Cultivation Fund, China, grant number GDMUQ2021004, GMUQ2021010; Zhanjiang Science And Technology Research Plan Project, grant number 2021B01454; Competitive Allocation Project Of Special Funds For Science And Technology Development Of Zhanjiang City, grant number 220829004544444.

Conflict of Interest

The authors declare no conflict of interest.

References

[1] Cai Z, Zhang J, Li H. Selenium, aging and aging-related diseases. Aging Clinical and Experimental Research. 2019; 31: 1035–1047.

[2] Gassen NC, Chrousos GP, Binder EB, Zannas AS. Life stress, glucocorticoid signaling, and the aging epigenome: implications for aging-related diseases. Neuroscience & Biobehavioral Reviews. 2017; 74: 356–365.

[3] Hooper SB, Wallace MJ. Role of the physicochemical environment in lung development. Clinical and Experimental Pharmacology and Physiology. 2006; 33: 273–279.
[4] Wang L, Green F, Smiley-Jewell S, Pinkerton K. Susceptibility of the Aging Lung to Environmental Injury. Seminars in Respiratory and Critical Care Medicine. 2010; 31: 539–553.
[5] Valavanidis A, Vlachogianni T, Fiotakis K, Loridas S. Pulmonary oxidative stress, inflammation and cancer: respirable particulate matter, fibrous dusts and ozone as major causes of lung carcinogenesis through reactive oxygen species mechanisms. International Journal of Environmental Research and Public Health. 2013; 10: 3886–3907.
[6] Risom L, Møller P, Loft S. Oxidative stress-induced DNA damage by particulate air pollution. Mutation Research/Fundamental and Molecular Mechanisms of Mutagenesis. 2005; 592: 119–137.
[7] Abarca ML, Accensi F, Bragulat MR, Cabañes FJ. Current Importance of Ochratoxin A–Producing Aspergillus spp. Journal of Food Protection. 2001; 64: 903–906.
[8] El Khoury A, Atoui A. Ochratoxin A: General overview and actual molecular status. Toxins. 2010; 2: 461–493.
[9] Raj J, Vasiljević M, Tassis P, Farkaš H, Bošnjak-Neumüller J, Männer K. Effects of a modified clinoptilolite zeolite on growth performance, health status and detoxification of aflatoxin B1 and ochratoxin An in male broiler chickens. British Poultry Science. 2021; 62: 601–610.
[10] Sorrenti V, Di Giacomo C, Acquaviva R, Barbagallo I, Bognanno M, Galvano F. Toxicity of ochratoxin A and its modulation by antioxidants: A review. Toxins. 2013; 5: 1742–1766.
[11] Markov K, Pleadin J, Bevardi M, Vahčić N, Sokolić-Mihalak D, Frece J. Natural occurrence of aflatoxin B1, ochratoxin a and citrinin in Croatian fermented meat products. Food Control. 2013; 34: 312–317.
[12] Imperato R, Campone L, Piccinelli AL, Veneziano A, Rastrelli L. Survey of aflatoxins and ochratoxin a contamination in food products imported in Italy. Food Control. 2011; 22: 1905–1910.
[13] Stoev, SD. Studies on carcinogenic and toxic effects of ochratoxin An in chicks. Toxins. 2010; 2: 649–664.
[14] Pfohl-Leszkowicz A, Manderville RA. Ochratoxin A: An overview on toxicity and carcinogenicity in animals and humans. Molecular Nutrition & Food Research. 2007; 51: 61–99.
[15] Dortant PM, Peters-Volleberg GWM, Van Loveren H, Marquardt RR, Speijers GJA. Age-related differences in the toxicity of ochratoxin An in female rats. Food and Chemical Toxicology. 2001; 39: 55–65.
[16] Al-Anati L, Petzinger E. Immunotoxic activity of ochratoxin A. Journal of Veterinary Pharmacology and Therapeutics. 2006; 29: 79–90.
[17] Frangiamone M, Cimbalo A, Alonso-Garrido M, Vila-Donat P, Manyes L. In vitro and in vivo evaluation of AFB1 and OTA-toxicity through immunofluorescence and flow cytometry techniques: a systematic review. Food and Chemical Toxicology. 2022; 160: 112798.
[18] Costa JG, Saraiva N, Guerreiro PS, Louro H, Silva MJ, Miranda JP, *et al*. Ochratoxin a-induced cytotoxicity, genotoxicity and reactive oxygen species in kidney cells: an integrative approach of complementary endpoints. Food and Chemical Toxicology. 2016; 87: 65–76.
[19] Le G, Yang L, Du H, Hou L, Ge L, Sylia A, *et al*. Combination of zinc and selenium alleviates ochratoxin a-induced fibrosis via blocking ROS-dependent autophagy in HK-2 cells. Journal of Trace Elements in Medicine and Biology. 2022; 69: 126881.
[20] Anderson LA, Goodman RA, Holtzman D, Posner SF, Northridge ME. Aging in the United States: opportunities and challenges for public health. American Journal of Public Health. 2012; 102: 393–395.
[21] Bui-Klimke TR, Wu F. Ochratoxin A and human health risk: A review of the evidence. Critical Reviews in Food Science and Nutrition. 2015; 55: 1860–1869.
[22] Giaimo S, d'Adda di Fagagna F. Is cellular senescence an example of antagonistic pleiotropy? Aging Cell. 2012; 11: 378–383.
[23] Zglinicki TV, Saretzki G, Ladhoff J, Fagagna FDD, Jackson SP. Human cell senescence as a DNA damage response. Mechanisms of Ageing and Development. 2005; 126: 111–117.
[24] de Magalhães JP, Passos JF. Stress, cell senescence and organismal aging. Mechanisms of Aging and Development. 2018; 170: 2–9.
[25] Ohtani N, Mann DJ, Hara E. Cellular senescence: its role in tumor suppression and aging. Cancer Science. 2009; 100: 792–797.
[26] Itahana K, Campisi J, Dimri GP. Mechanisms of cellular senescence in human and mouse cells. Biogerontology. 2004; 5: 1–10.
[27] Salminen A, Kauppinen A, Kaarniranta K. Emerging role of NF-κB signaling in the induction of senescence-associated secretory phenotype (SASP). Cellular Signalling. 2012; 24: 835–845.
[28] Liochev SI. Reactive oxygen species and the free radical theory of aging. Free Radical Biology and Medicine. 2013; 60: 1–4.
[29] Simon HU, Haj-Yehia A. Levi-Schaffer F. Role of reactive oxygen species (ROS) in apoptosis induction. Apoptosis. 2020; 5: 415–418.
[30] Longobardi C, Damiano S, Andretta E, Prisco F, Russo V, Pagnini F, *et al*. Curcumin modulates nitrosative stress, inflammation, and DNA damage and protects against ochratoxin A-induced hepatotoxicity and nephrotoxicity in rats. Antioxidants. 2021; 10: 1239.
[31] Damiano S, Longobardi C, Andretta E, Prisco F, Piegari G, Squillacioti C, *et al*. Antioxidative effects of curcumin on the hepatotoxicity induced by ochratoxin a in rats. Antioxidants. 2021; 10: 125.
[32] Longobardi C, Ferrara G, Andretta E, Montagnaro S, Damiano S, Ciarcia R. Ochratoxin A and Kidney Oxidative Stress: The Role of Nutraceuticals in Veterinary Medicine—A Review. Toxins. 2022; 14: 398.
[33] Wang Y, Cui J, Zheng G, Zhao M, Hao Z, Lian H, *et al*. Ochratoxin a induces cytotoxicity through ROS-mediated endoplasmic reticulum stress pathway in human gastric epithelium cells. Toxicology. 2022; 479: 153309.
[34] Longobardi C, Ferrara G, Andretta E, Montagnaro S, Damiano S, Ciarcia R. Ochratoxin A and Kidney Oxidative Stress: The Role of Nutraceuticals in Veterinary Medicine—A Review. Toxins. 2022; 14: 398.
[35] García-Pérez E, Ryu D, Lee C, Lee HJ. Ochratoxin A induces oxidative stress in HepG2 Cells by impairing the gene expression of antioxidant enzymes. Toxins. 2021; 13: 271.
[36] Il'ichev YV, Perry JL, Simon JD. Interaction of ochratoxin A with human serum albumin. Preferential binding of the dianion and pH effects. The Journal of Physical Chemistry B. 2002; 106: 452–459.